International Journal of Minerals, Metallurgy and Materials
Volume 29, Number 2, February 2022, Page 218
https://doi.org/10.1007/s12613-020-2161-6

Process and kinetics of the selective extraction of cobalt from high-silicon low-grade cobalt ores using ammonia leaching

Lei Tian[*], *Ao Gong*[*], *Xuangao Wu*, *Xiaoqiang Yu*, *Zhifeng Xu*[✉], *and Lijie Chen*[✉]

Institute of Green Metallurgy and Process Intensification, Jiangxi University of Science and Technology, Ganzhou 341000, China
(Received: 9 April 2020; revised: 4 August 2020; accepted: 6 August 2020)

Abstract: An ammonia-based system was used to selectively leach cobalt (Co) from an African high-silicon low-grade Co ore, and the other elemental impurities were inhibited from leaching in this process. This process was simple and environmentally friendly. The results revealed that the leaching ratio of Co can reach up to 95.61% using $(NH_4)_2SO_4$ as a leaching agent under the following materials and conditions: $(NH_4)_2SO_4$ concentration 300 g/L, reductant dosage 0.7 g, leaching temperature 353 K, reaction time 4 h, and liquid–solid ratio 6 mL/g. The leaching kinetics of Co showed that the apparent activation energy of Co leaching was 76.07 kJ/mol (i.e., in the range of 40–300 kJ/mol). This indicated that the leaching of Co from the Co ore was controlled by an interfacial chemical reaction, and then the developed leaching kinetics model of the Co can be expressed as $1-(1-\alpha)^{1/3}=28.01\times10^3\times r_0^{-1}\times C_{(NH_4)_2SO_4}^{1.5}\times\exp(-76073/8.314T)\times t$, where α is the leaching ratio (%) of Co, r_0 is the average radius (m) of the Co ore particles, T is the temperature (K), and $C_{(NH_4)_2SO_4}$is the initial reactant concentration (kg/m^3).

Keywords: ammonia leaching; leaching kinetics; selective extraction; cobalt

1. Introduction

Co is a strategic metal widely used for various types of applications, such as in defense industries, alloy materials, catalysts, battery materials, and automobile industries, because of its excellent physicochemical properties [1–4]. Developments in science and technology have increased the demand for the Co metals each year [5–8]. But Co resources are relatively scarce in China. Further, only are the low-grade Co ores available, and they are mostly combined with other ores, which makes the extraction of Co very difficult. Moreover, Co ores have a complex composition, and their processing is complicated. In addition, the recovery ratio of Co is low [9–11].

Most methods used for treating Co ores involve acid leaching, which has been used in the industry. However, there are persistent problems in acid leaching. It not only leaches Co but also other elemental impurities present. Moreover, the subsequent purification and impurity removal processes are cumbersome, and a large amount of alkali is consumed in the waste liquid treatment leading to increased costs. In addition, the sulfate waste produced during leaching can affect the environment adversely [12–14].

Previous studies showed that ammonia leaching has been widely used to extract valuable metals such as copper and zinc from ores or waste materials [15–19]. Chen *et al*. [20] used ammonia leaching to extract valuable metals from waste cathode materials. The experimental results indicated that after roasting the waste cathode materials under optimum conditions, which involved the use of 3 M $(NH_4)_2SO_4$, 0.75 M $(NH_4)_2SO_3$, and a solid to liquid ratio (S : L) of 83 g/L, the leaching ratio of Ni, Li, Co, and Mn can reach 98%, 98%, 81%, and 92%, respectively. Wu *et al*. [21] used a ternary leaching system consisting of NH_3, $(NH_4)_2SO_3$, and NH_5CO_3 to recover valuable elements from waste lithium-ion batteries. In their study, the following compounds and parameters were used in the process under optimum conditions: ammonia 1.5 M, ammonium sulfite 1 M, and ammonium bicarbonate 1M, at 60°C; pulp density of 20 g/L; leaching time of 180 min. Using these materials with the optimum conditions, the Ni and Cu are nearly completely leached out. Qi *et al*. [22] used ammonia leaching to extract cobalt and lithium from waste lithium-ion batteries; under the best conditions ($NH_3\cdot H_2O$ 120 g/L; NH_4HCO_3 75 g/L; the molar ratio of Na_2SO_3 to Co = 2:1; 353 K; 240 min), the leaching ratios of Co and Li are found to be 91.16% and 97.57%, respectively. It is found out from the kinetic study that the speed-limiting step of the leaching process is the interfacial chemical reaction. Oluokun and Otunniyi [23] used the ammonia oxidation leaching method to treat the waste circuit board dust. The mixed solution of 2 M NH_4OH and 17.5 M H_2O_2 was used as the leaching agent under the experimental conditions of 313 K, 101325 Pa, and 400 r/min to process the dust with a particle size of 75–106 μm, the recovery ratios of copper and zinc can

[*] These authors contributed equally to this work.

✉ Corresponding authors: Zhi-feng Xu E-mail: xu.zf@jxust.edu.cn; Li-jie Chen E-mail: 81191520@qq.com

reach up to 92% and 50% respectively.

The above studies have shown that when using the ammonia leaching method to extract valuable metals, Cu and Co react with ammonia to form a complex $[Me(NH_3)_i]^{2+}$ (Me = Cu, Co; *i* is the coordination number of NH_3), which enters the leaching solution. However, most elemental impurities, such as Ca, Fe, and Si, do not react with ammonia and remain as the gangue components, and so they can be separated from the target metal easily. The leaching solution has fewer impurities, and consequently, the purification process is simple and short. Cu and Co are extracted and separated from the leachate under the ammonia system that can effectively avoid various problems encountered in the acidic system. Ammonia and ammonium salts can be recycled from waste liquid produced during leaching after ammonia evaporation, and in theory, the complete recycle of raw materials can be achieved, which result in emission reduction, cost efficiency, and environmental friendliness [24–26].

To achieve economic viability and environmental protection, a mmonia leaching was used to investigate the efficient and selective extraction of Co from the high-silicon low-grade Co ore, and the ammonia-based leaching agent were simultaneously recycled in this study.

2. Experimental

2.1. Materials and pretreatment

The raw material used in the experiment was a high-silicon low-grade Co ore from Africa. The ore was dried at 80°C for 24 h to determine the phase and chemical composition of the ore. It was then analyzed using inductively coupled plasma optical emission spectroscopy (ICP-OES), X-ray photoelectron spectroscopy (XRF), scanning electron microscope (SEM), and energy dispersive spectrometer (EDS). Table 1 presents the chemical composition of the high-silicon low-grade Co ore. The main constituents of the high-silicon low-grade Co ore are Si, Ca, Mg, Al, and O, but the content of Co is low (0.29wt%).

The pattern generated by X-ray diffraction (XRD) of the high-silicon low-grade Co ore is presented in Fig. 1, which shows that the main phases of the high-silicon low-grade Co ore are SiO_2, $CaMg(CO_3)_2$, and $MgAl_2O_4$.

Table 1. Main chemical components of the low-grade Co ore

wt%

Co	O	Fe	Si	Cu	S	Ca	Ti	Mg	Al
0.29	33.18	0.86	25.48	1.22	0.02	6.38	0.23	4.07	3.24

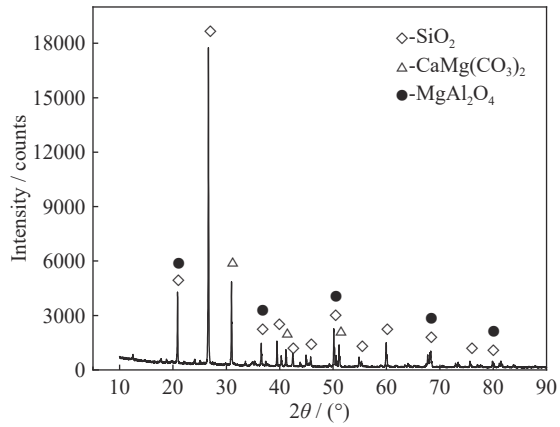

Fig. 1. XRD pattern of the low-grade Co ore.

SEM–EDS analysis of the high-silicon low-grade Co ore was performed to analyze the particle morphology and elemental distribution of the high-silicon low-grade Co ore. The images obtained during the SEM–EDS analysis are presented in Fig. 2. The approximate size of the Co ore particle is 10 μm, and the particles has a smooth surface. In addition, Mg, Al, Si, and other elements are mostly combined with oxygen in the form of oxides, and their Co contents are low; this result is consistent with the results of XRD analysis and chemical composition analysis.

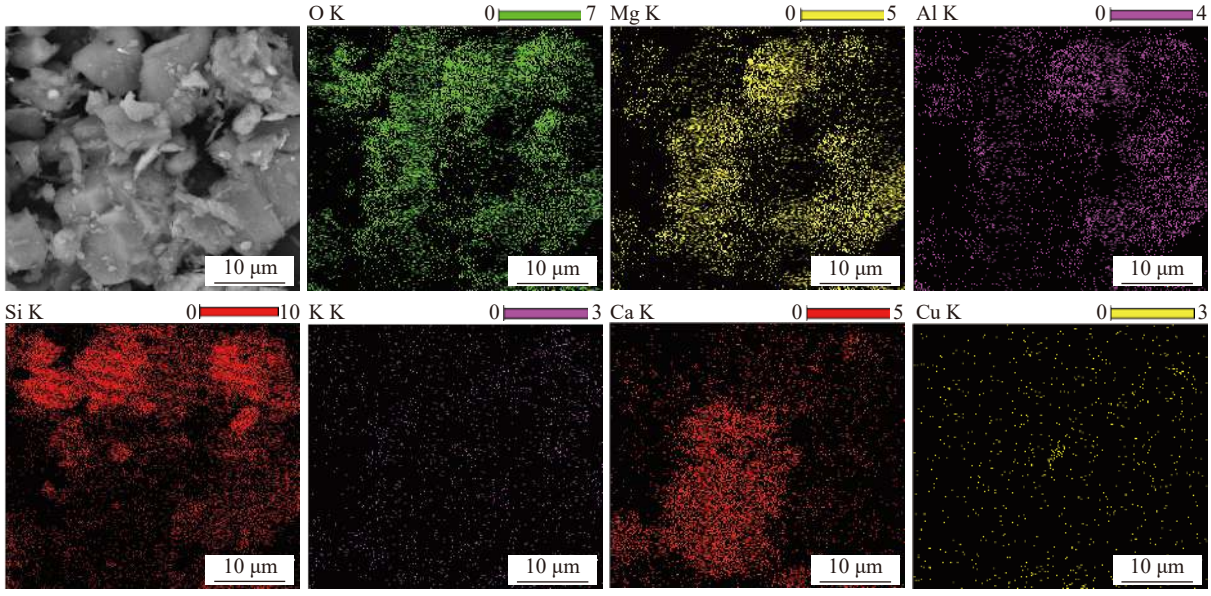

Fig. 2. SEM–EDS images of the low-grade Co ore.

2.2. Procedure

2.2.1. Single-factor experiment

The raw material and leaching agent were mixed in a certain liquid–solid ratio and heated at a certain temperature. Single-factor experiments were used to examine the various factors such as leaching agent concentration, reducing agent dosage, temperature, reaction time, and liquid–solid ratio. The leach residue and leachate obtained during the experiment were subjected to a phase and elemental composition analysis. The experimental flow chart is presented in Fig. 3, the experimental instrument models are: QM-2-A type drum ball mill, XSB-88 top impact type standard vibrating screen machine, and DF-101S collector type constant temperature heating magnetic stirrer. The leaching ratio of Co was calculated by the following equation:

$$\alpha = \frac{C_1 \times V_1}{m_0 \times x_0} \times 100\% \quad (1)$$

where α is the metal (Co) leaching efficiency (%); C_1 is the concentration of Co in the leach liquor (g/L); V_1 is the leach liquor volume (L); m_0 is the initial mass of the sample (g); x_0 is the content of Co in the sample (wt%).

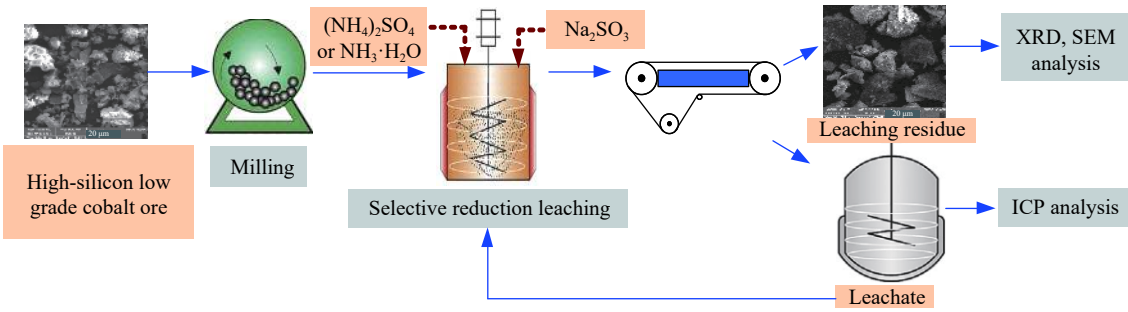

Fig. 3. Flowchart illustrating the selective reduction ammonium leaching of the low-grade Co ore.

2.2.2. Kinetic experiment

$(NH_4)_2SO_4$ solution (300 mL), high-silicon low-grade Co ore (10.0 g), and an appropriate amount of Na_2SO_3 were added to the heat-collecting reactor and heated to a set temperature. Then, 5 mL of the leaching solution was taken out at predetermined time intervals, and the concentration of the elemental ions was analyzed. Finally, fitting was carried out to obtain the relevant kinetic parameters and equations.

2.3. Analysis of reaction mechanism

During the ammonia leaching of the Co ore, Co^{2+} forms complexes with ammonia, whereas other elements do not react with Co and ammonia. Thus, the selective extraction of Co was achieved. The main reactions that occur during leaching are represented by the following equation:

$$Co^{2+} + iNH_3 = Co(NH_3)_i^{2+} \quad (2)$$

where i in the complex $Co(NH_3)_i^{2+}$ depends upon the molar ratio of NH_3 and Co and is found to be in the range of 1–6. Table 2 shows the stability constants of the ammonia complex ions of Co [27]. The stability of the complex gradually increases with increase in i. The analysis of the complexation reaction is shown in Fig. 4. In addition, $Co(OH)_3$ and $Co(OH)_2$ may be formed during the ammonia leaching process, and the solubility product constant (K_{sp}) of $Co(OH)_3$ is much smaller than $Co(OH)_2$ (K_{sp} of $Co(OH)_3$ is 3.0×10^{-41}, K_{sp} of $Co(OH)_2$ is 6.0×10^{-15}) [28–29]. To avoid excessive formation of $Co(OH)_3$ precipitation in the leaching process, which may result in the loss of cobalt, the reducing agent

Table 2. Stability constants (β_i) of the cobalt–ammonia complexation ion

Specie	$\lg\beta_i$	Specie	$\lg\beta_i$
$Co(NH_3)^{2+}$	2.11	$Co(NH_3)_4^{2+}$	5.55
$Co(NH_3)_2^{2+}$	3.74	$Co(NH_3)_5^{2+}$	5.73
$Co(NH_3)_3^{2+}$	4.79	$Co(NH_3)_6^{2+}$	5.11

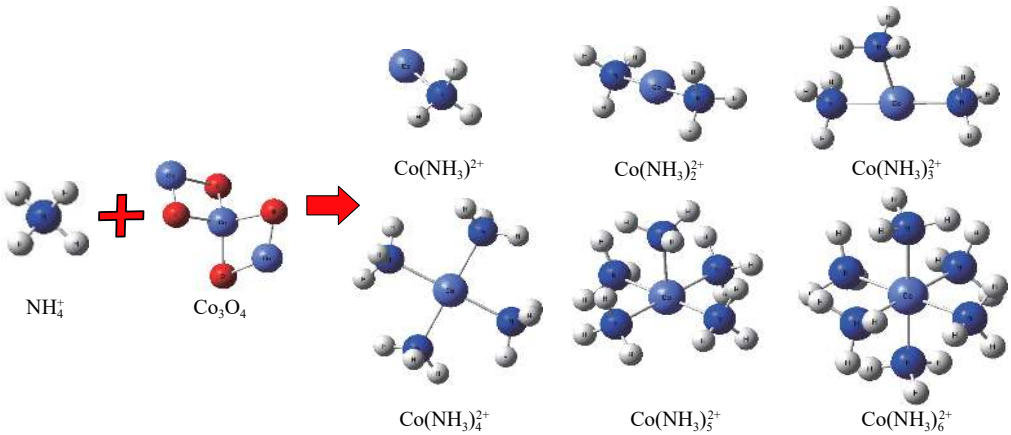

Fig. 4. Analysis of the complexation reaction.

Na_2SO_3 was added in this study to improve the leaching ratio of cobalt.

3. Results and discussion

3.1. Optimal conditions for ammonia leaching experiment

3.1.1. Leaching agent selection

The effects of ammonia water (7 mol/L) and $(NH_4)_2SO_4$ solution (300 g/L) on the Co leaching ratio were investigated at a temperature of 353 K, liquid–solid ratio (L/S) of 6 mL/g, Na_2SO_3 of 0.7 g, stirring rate of 400 r/min, and leaching time of 4 h when the particle sizes of ore is at the range of 45–75 μm. The experiment was performed three times for both leaching agents to minimize the error and results of analysis were obtained. Table 3 shows the comparative results. It is found from experimental data that the extracting efficiency of cobalt with ammonium sulfate leaching process is higher. In addition, it was also observed by Liu *et al*. [30] that the reduction potential of the reducing agent decreases as the pH of the solution increases, which is not conducive to the leaching of cobalt from the ore. Moreover, ammonia is volatile and the working environment will become dangerous, so ammonium sulfate was selected as the leaching agent.

Table 3. Co leaching ratios of three experiments under every leaching agent %

Leaching agent type	First time	Second time	Third time	Average of three experiments
Ammonia	90.28	91.36	90.55	90.73
Ammonium hydrogen sulfate	95.32	94.96	95.25	95.70

3.1.2. Effect of single-factor on the Co leaching ratio

In the single-factor tests, when one factor value is changed, the other factors in the leaching system maintain the following conditions unchanged: temperature of 353 K, $(NH_4)_2SO_4$ concentration of 300 g/L, Na_2SO_3 amount of 0.7 g, L/S of 6 mL/g, particle-size range of 45–75 μm, and leaching time of 4 h. The results of all single-factor tests are shown in Fig. 5.

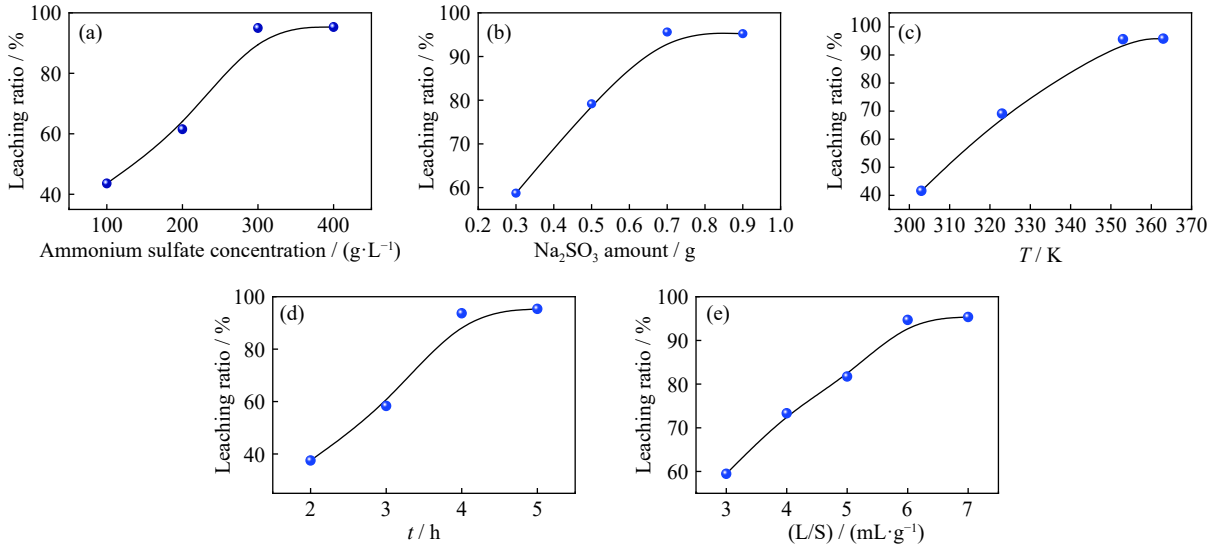

Fig. 5. Effect of $(NH_4)_2SO_4$ concentration (a), Na_2SO_3 amount (b), leaching temperature *T* (c), leaching time *t* (d), and liquid–solid ratio (e) on the Co leaching ratio.

As shown in Fig. 5(a), when the concentrations of $(NH_4)_2SO_4$ less than 300 g/L, the leaching ratio of Co increases with the increase in concentration of $(NH_4)_2SO_4$. When the concentration of $(NH_4)_2SO_4$ reaches 300 g/L, the leaching ratio of Co reaches the maximum value of 95.61%. Further increase in the concentration of $(NH_4)_2SO_4$ does not affect the leaching ratio of Co and it remains unchanged because when the concentration of $(NH_4)_2SO_4$ reaches 300 g/L, the leaching of Co is relatively over. So, a further increase in the concentration of $(NH_4)_2SO_4$ does not increase the leaching ratio of Co significantly. Fig. 5(b) shows that the leaching ratio of Co increases with increase in Na_2SO_3 dosage, illustrating the vital role of Na_2SO_3 in the reduction. The leaching ratio of Co reaches the maximum value of 95.61% when the Na_2SO_3 dosage is 0.7 g. Further, the leaching ratio of Co remains more or less constant when the dosage of Na_2SO_3 is further increases. Therefore, it is considered appropriate to maintain the dosage of Na_2SO_3 at 0.7 g. In Fig. 5(c), the leaching ratio of Co increases with increasing temperature, which indicates the importance of temperature in increasing the leaching ratio of Co. After the temperature higher than 353 K, the leaching ratio changed insignificantly. Therefore, the temperature is maintained at 353 K. As the leaching time increases, the leaching ratio of Co also gradually increases till the time 4 h, which will be its maximum value (Fig. 5(d)). Further, when the leaching time exceeds 4 h, the leaching ratio of Co remained unchanged. As shown in Fig. 5(e), the Co leaching ratio also increases with the increase of the liquid–solid ratio.

It is observed that when liquid–solid ratios are low, the contact between $(NH_4)_2SO_4$ and Co ore is insufficient, mobility of ions is less, and Co in the leaching solution gets easily saturated. In addition, when the liquid–solid ratio reaches higher than 6 g/L, the leaching ratio remains unchanged.

Out of all of above results, the optimal condition of ammonia leaching for the high-silicon low-grade cobalt ores is determined as follows: temperature of 353 K, $(NH_4)_2SO_4$ concentration of 300 g/L, Na_2SO_3 amount of 0.7 g, L/S of 6 mL/g, particle-size range of 45–75 μm, and leaching time of 4 h.

3.2. Phase change of the leaching residue

The chemical composition of the leaching slag of high-silicon low-grade cobalt ore is shown in Table 4. Compared with Table 1, it can be observed that the content of Cu and Co in the leaching slag is significantly reduced, and the quantity of other elements remains unchanged, indicating that Cu and Co are selectively leached into the solution. The obtained leach liquor can be further treated by the extraction or ion exchange to separate and recover copper and cobalt metals.

Table 4. Main chemical components of leaching slag wt%

Co	O	Fe	Si	Cu	S	Ca	Ti	Mg	Al
0.01	32.07	0.88	25.85	0.03	0.03	6.32	0.33	3.92	3.42

XRD pattern was used to analyze the ammonia leaching residue and the obtained results are presented in Fig. 6. The main phases existing in the leaching residue are SiO_2, $CaMg(CO_3)_2$, and $MgAl_2O_4$. This observation is consistent with the composition of the raw material discussed earlier. It also indicates that the ammonia leaching does not cause any structural damage to the phases of compounds in the crude ore.

The SEM–EDS images of the leaching residue are displayed in Fig. 7. The leaching residue particles are relatively uniform and few small-sized particles or flake-like particles are also observed. The EDS analysis reveals that the distribution of each element in the leaching residue is relatively concentrated, and the distribution areas of silicon and oxygen are similar. This indicates that Si in the leaching residue particles mainly is in the form of SiO_2, and the distribution areas of calcium, magnesium, and oxygen are also similar, which indicate the occurrence of a calcium–magnesium spinel phase. This observation is similar to the results of the EDS analysis of the low-grade Co ore particles.

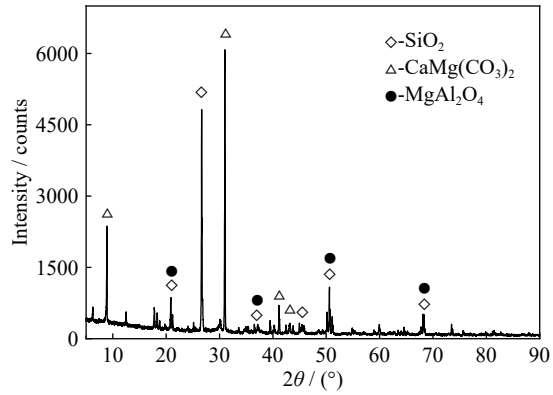

Fig. 6. XRD pattern of leaching residue.

3.3. Cycle test results

Through single-factor experiments, we obtained the optimal experimental conditions for leaching Co. Afterwards, we conducted leachate recirculation experiments to explore the economic feasibility of ammonia leaching for cobalt extraction. Firstly, the cobalt ore was ammonia leached under an optimal process conditions ($(NH_4)_2SO_4$ concentration of 300 g/L, Na_2SO_3 addition amount of 0.7 g, reaction temperature of 353 K, reaction time of 4 h, and L/S of 6 mL/g), and the leachate obtained was supplemented with appropriate amount of Na_2SO_3 and then could be reused as leaching agent to extract Co from cobalt ore. The cycle of leaching was repeated four times and the leaching ratio of Co was calculated respectively.

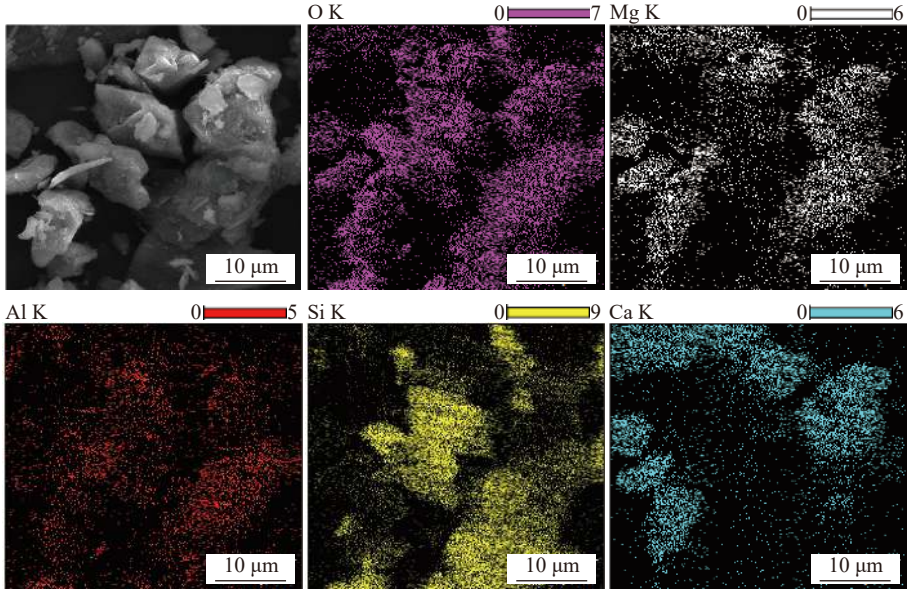

Fig. 7. SEM–EDS images of the leaching residue.

The results for the leaching ratio after four cycles of testing are shown in Fig. 8. The leaching ratio of Co insignificantly reduces and remains almost unchanged after four cycles, which are remains in the range of 95.31%–95.72%. It indicates that when $(NH_4)_2SO_4$ is used as the leaching agent to treat the low-grade Co ore, the leachate can be recycled and reused. This proves that the leaching process investigated in this study can be economically beneficial.

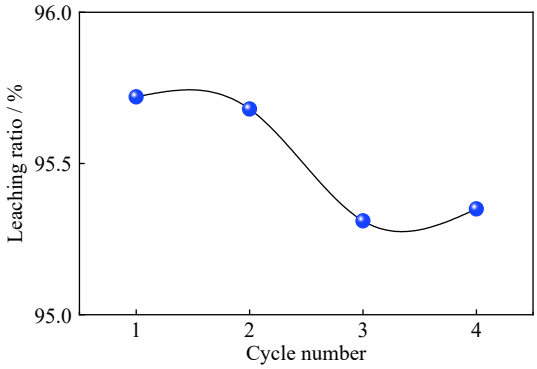

Fig. 8. Results of the cycle experiment.

3.4. Kinetics analysis

It is already known that a liquid–solid reaction occurrs at the interface between the two phases during the ammonia leaching of the Co ores. During leaching, a product layer with loose texture is formed. Reactants may diffuse to the new reaction interface through the tiny pores and channels on the product layer. The products can also enter the solution through the pore channels of the product layer.

The equation for the leaching kinetics of the unreacted shrinking core model with the solid product layer is expressed as [31–34]:

$$\frac{\delta\alpha}{3D_1}+\frac{r_0}{2D_s}\left[1-\frac{2}{3}\alpha-(1-\alpha)^{\frac{2}{3}}\right]+\frac{1}{k_r}\left[1-(1-\alpha)^{\frac{1}{3}}\right]=\frac{C_{A0}}{4\rho r_0}t \tag{3}$$

where δ is the thickness (m) of the boundary layer; D_1 is the mass transfer coefficient (m/s) in the boundary layer; α is the leaching ratio (%) of Co; r_0 is the initial radius (m) of the Co ore particles; D_s is the mass transfer coefficient (m/s) of the solid product layer; k_r is the interfacial reaction rate constant; C_{A0} is the initial reactant concentration (kg/m^3); ρ is the density (kg/m^3) of the Co ore; t is the reaction time (min).

When $r_0/(2D_s) \gg \delta/(3D_1)$ and $r_0/(2D_s) \gg k_r^{-1}$, the solid product layer diffusion is the main controlling process, and the equation can be simplified as follows:

$$1-\frac{2}{3}\alpha-(1-\alpha)^{\frac{2}{3}}=\frac{D_sC_{A0}}{2\rho r_0^2}t=kt \tag{4}$$

where k is the rate constant.

When $k_r^{-1} \gg \delta/(3D_1)$ and $k_r^{-1} \gg r_0/(2D_s)$, the total interface chemical reaction is the main controlling process, and the equation can be simplified as follows:

$$1-(1-\alpha)^{\frac{1}{3}}=\frac{k_rC_{A0}}{4\rho r_0}t=kt \tag{5}$$

The Arrhenius equation is

$$k=A_0\exp\left(\frac{-E}{RT}\right) \tag{6}$$

where k is the rate constant, R = 8.314 J·mol^{-1}·K^{-1}, T is the temperature (K), E is the apparent activation energy (J/mol), and A_0 is the pre-exponential factor.

To investigate the kinetics of leaching, the experimental conditions must meet kinetic requirements; therefore, the L/S must be high. The kinetic experiments in this study were conducted at an L/S of 30 mL/g. Other factors were set to obtain the best conditions as described above.

3.4.1. Leaching regular pattern under different reaction temperatures

Fig. 9 shows the effect of temperature on the Co leaching. The leaching ratio of Co obtained at different temperatures were used in Eqs. (4) and (5) to determine the control steps of the Co leaching process, and the fitting results are presented in Fig. 10.

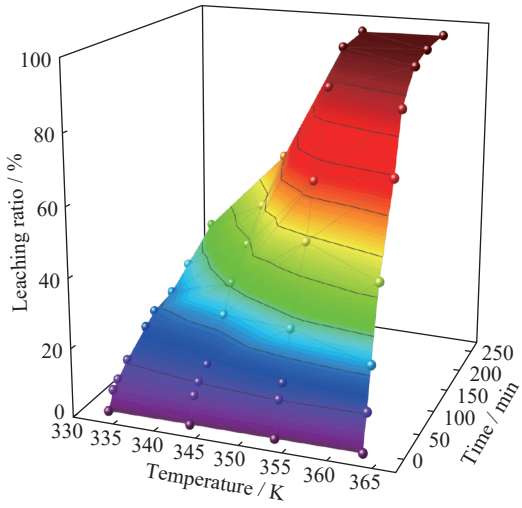

Fig. 9. Effect of temperature on the Co leaching ratio.

The fitting results in Fig. 10 indicate that the fitting effect of Fig. 10(b) is better than that of Fig. 10(a). Then, the natural logarithm ln k obtained from the slope of the fitting straight line in Fig.10(a) and (b) was plotted against $1/T$ and the relationship is presented in Fig. 11.

The fitting degree of Fig.11(b) is significantly higher than that of Fig.11(a), and the activation energy obtained by Fig.11(a) fitting is 123.13 kJ/mol, which dose not conform to diffusion control (diffusion control activation energy is generally less than 13 kJ/mol). Fig. 11(b) indicates that ln k has a good linear relationship with $1/T$, and the correlation coefficient is found to be R^2 = 0.94. According to the Arrhenius formula, the leaching activation energy of Co is 76.07 kJ/mol, which is in the range of 40–300 kJ/mol; therefore, it can be understood that the process of leaching Co from the Co ore is controlled by the interface chemical reaction [35]. Therefore, model of Eq. (5) was adopted to describe the dissolution of Co ore in ammonium sulfate solution with sodium sulfite.

3.4.2. Leaching regular pattern under different particle sizes

The effect of particle size on Co leaching is shown in Fig.

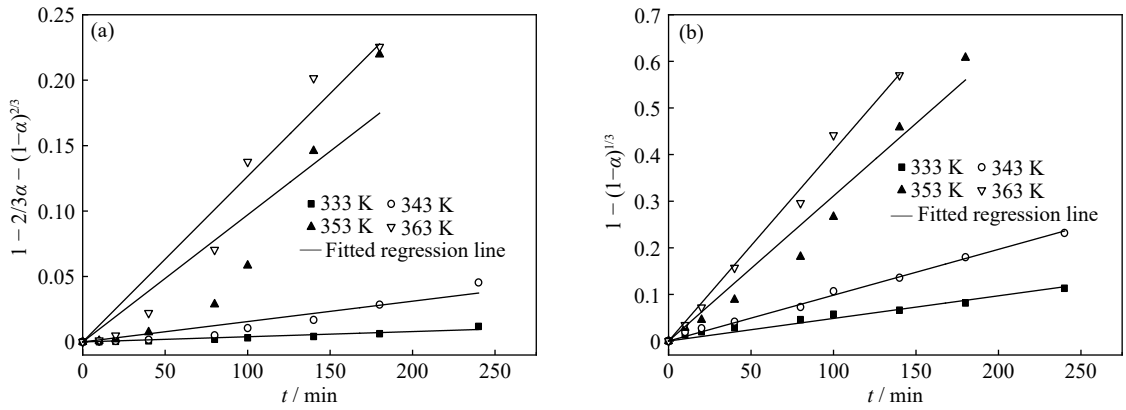

Fig. 10. Plot of (a) $1-2/3\alpha-(1-\alpha)^{2/3}$ and (b) $1-(1-\alpha)^{1/3}$ versus t for the Co leaching ratio at different temperatures.

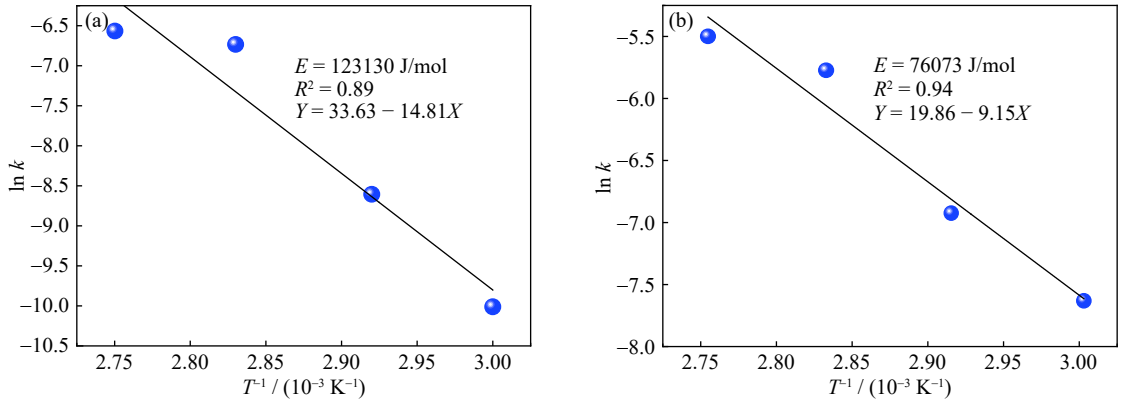

Fig. 11. Relationships between ln k and T^{-1} when the rate for Co leaching is controlled by different processes: (a) controlled by the solid product layer diffusion; (b) controlled by the interface chemical reaction.

12. It is evident that the leaching ratio of Co increases with decreasing particle size. This indicates that, within a certain particle size range, a small particle size facilitates sufficient contact with ammonium sulfate to promote leaching. A serious well-fitted plots of $1-(1-\alpha)^{1/3}$ versus time at different particle size ranges was given in Fig. 13. According to the slope K of each fitting straight line in Fig. 13, the k and $1/r_0$ were fitted, as shown in Fig. 14. According to the fitting result in Fig. 14, empirical order of reaction with particle size is about 0.21.

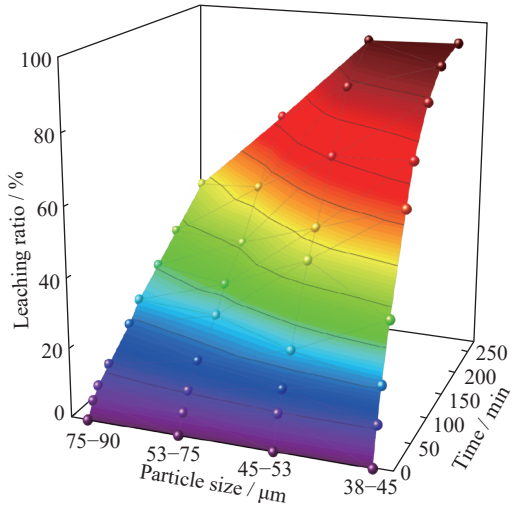

Fig. 12. Effect of particle size on the extraction of Co.

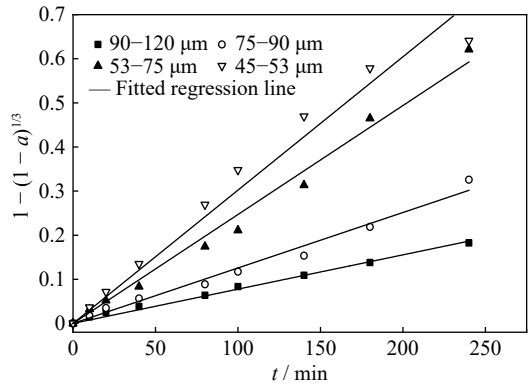

Fig. 13. Straight line of $1-(1-\alpha)^{1/3}$ and t at different particle sizes.

3.4.3. Leaching regular pattern under ammonium sulfate concentrations

Fig. 15 shows the effect of the ammonium sulfate concentration ($C_{(NH_4)_2SO_4}$) on Co leaching. A serious well-fitted plots of $1-(1-\alpha)^{1/3}$ versus time at different ammonium sulfate was given in Fig. 16. According to the slope K of each fitting straight line in Fig. 16, the natural logarithms ln k and ln$C_{(NH_4)_2SO_4}$ were fitted, as shown in Fig. 17. According to the fitting result in Fig. 17, empirical orders of reaction with ammonium sulfate concentrations is about 1.50, because 1.50 > 1, indicating that increasing the concentration of ammonium sulfate is conducive to accelerating the reaction.

3.4.4. Establishment of a dynamic model

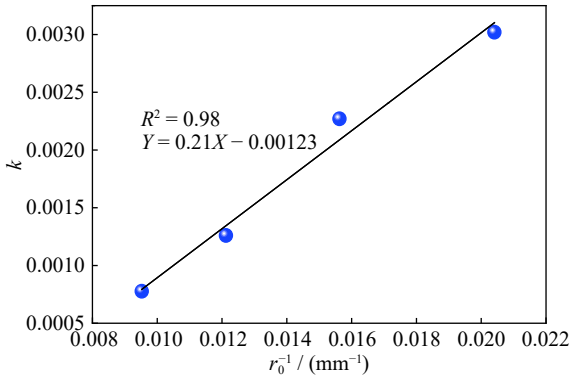

Fig. 14. Fit line for k and $1/r_0$.

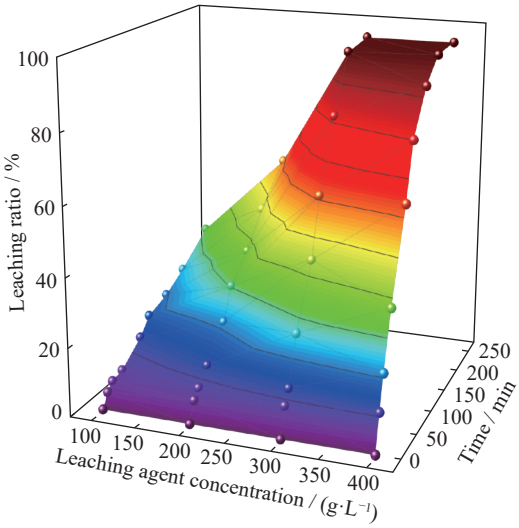

Fig. 15. Effect of leaching agent concentration on Co leaching ratio.

The control parameters used in the present work, including temperature, particle size, ammonium sulfate concentration were applied to developing the kinetics model. Combined with the above calculations, the effects of all the factors on the rate constant can be expressed as follows:

$$k = k_0 \times 0.21 r_0^{-1} \times C_{(NH_4)_2SO_4}^{1.5} \times \exp\left(\frac{-76073}{8.314T}\right) \quad (7)$$

Comparing Eq. (5) with Eq. (7), the dissolution kinetics of cobalt ore can be expressed as follows:

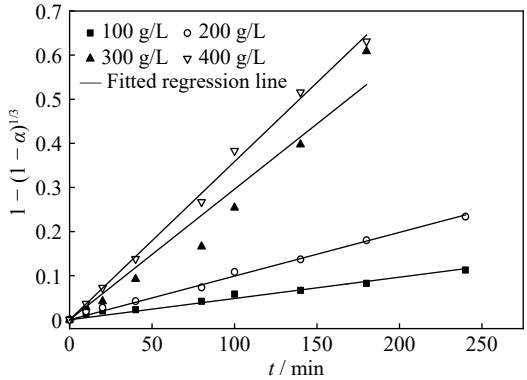

Fig. 16. Straight line of $1-(1-\alpha)^{1/3}$ and t at different leaching agent concentrations.

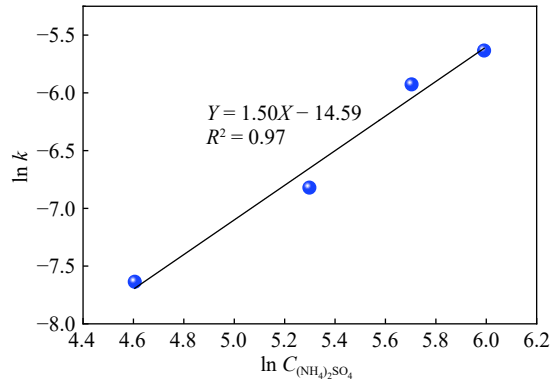

Fig. 17. Fitting relationship between ln k and ln $C_{(NH_4)_2SO_4}$.

$$1-(1-\alpha)^{\frac{1}{3}} = kt = k_0 \times 0.21 r_0^{-1} \times C_{(NH_4)_2SO_4}^{1.5} \times \exp\left(\frac{-76073}{8.314T}\right) \times t \quad (8)$$

where k_0 is constant.

The fitting relationship between $1-(1-\alpha)^{1/3}$ and $0.21 r_0^{-1} \times C_{(NH_4)_2SO_4}^{1.5} \times \exp\left(\frac{-76073}{8.314T}\right) \times t$ is shown in Fig. 18. Based on Fig. 18, k_0 is 133.38×10^3. Finally, the kinetic equation of the Co extraction can be expressed as:

$$1-(1-\alpha)^{\frac{1}{3}} = kt = 28.01 \times 10^3 \times r_0^{-1} \times C_{(NH_4)_2SO_4}^{1.5} \times \exp\left(\frac{-76073}{8.314T}\right) \times t \quad (9)$$

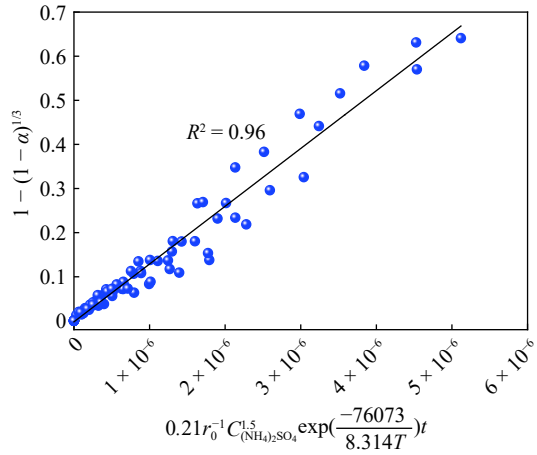

Fig. 18. Fitting relationship between $1-(1-\alpha)^{1/3}$ and $0.21 r_0^{-1} \times C_{(NH_4)_2SO_4}^{1.5} \times \exp\left(\frac{-76073}{8.314T}\right) \times t$.

4. Conclusions

A high-silicon low-grade Co ore and $(NH_4)_2SO_4$ solution were used as the raw material and leaching agent, respectively in our study. The effects of the addition of sodium sulfite, temperature, time, $(NH_4)_2SO_4$ concentration, and liquid–solid ratio on the Co extraction ratio were investigated. The kinetics of the Co leaching was further studied, and the kinetics model for the leaching of Co during the reductive ammonia leaching of high-silicon low-grade Co ore was obtained. The conclusions of this study are summarized as follows.

(1) During the reductive ammonia leaching of the high-sil-

icon low-grade Co ore, the leaching effect of $(NH_4)_2SO_4$, which was used as a leaching agent, was better than that of ammonia water. The maximum Co leaching ratio of 95.61% was achieved at a temperature of 353 K, $(NH_4)_2SO_4$ concentration of 300 g/L, L/S of 6 mL/g, and reaction time of 4 h, along with the addition of 0.7 g of Na_2SO_3 at an ore's particle-size range of 45–75 μm.

(2) The XRD analysis divulged that the main phases of the reduced ammonia leaching slag were SiO_2, $CaMg(CO_3)_2$, and $MgAl_2O_4$; this was consistent with the composition of the original Co ore. This indicated that the reduced ammonia leaching did not cause any structural damage to the phases existing in the ore. The SEM–EDS results indicated that the distribution of elements of the leaching slag was relatively concentrated, and the distribution areas of silicon and oxygen were approximately similar. This further proved that Si in the leaching residue particles was mainly in the form of SiO_2. The distribution areas of Ca, Mg, and O were also similar, which indicated the existence of a calcium-magnesium spinel phase. It was also noted that a similar result was obtained from the EDS analysis of the original ore. This indicated that Co leached into the $(NH_4)_2SO_4$ solution, thereby achieving selective leaching.

(3) The kinetic model analysis revealed that the activation energy of Co leaching was 76.07 kJ/mol (i.e., in the range of 40–300 kJ/mol), which indicated that the leaching process of Co in the high-silicon low-grade Co ore was controlled by an interfacial chemical reaction. The developed leaching kinetic model of Co in this study was represented by the equation given below: $1-(1-\alpha)^{\frac{1}{3}} = kt = 28.01\times10^3\times r_0^{-1}\times C_{(NH_4)_2SO_4}^{1.5}\times \exp\left(\frac{-76073}{8.314T}\right)\times t$.

Acknowledgements

This work was financially supported by the National Nature Science Foundation of China (Nos. 51804136, 52064021, 51974140, and 52064018), the Key Projects of Jiangxi Key R&D Plan, China (No. 20192ACB70017), the Jiangxi Provincial Cultivation Program for Academic and Technical Leaders of Major Subjects, China (No. 20204 BCJL23031), the Jiangxi Province Science Fund for Distinguished Young Scholars, China (No. 20202ACB213002), the Program of Qingjiang Excellent Young Talents, Jiangxi University of Science and Technology, China (JXUSTQJBJ 2020004), and the Distinguished Professor Program of Jinggang Scholars in institutions of higher learning, Jiangxi Province, China.

Conflict of Interest

Authors declare no potential conflict of interest.

References

[1] F.K. Crundwell, N.B. du Preez, and B.D.H. Knights, Production of cobalt from copper-cobalt ores on the African Copperbelt - An overview, *Miner. Eng.*, 156(2020), art. No. 106450.

[2] Kuzhipadath Jithesh and M. Arivarasu, Comparative studies on the hot corrosion behavior of air plasma spray and high velocity oxygen fuel coated Co-based L605 superalloys in a gas turbine environment, *Int. J. Miner. Metall. Mater.*, 27(2020), No. 5, p. 649.

[3] S. Iravani and R.S. Varma, Sustainable synthesis of cobalt and cobalt oxide nanoparticles and their catalytic and biomedical applications, *Green. Chem.*, 22(2020), No. 9, p. 2643.

[4] S.L. Zhang, W.Y. Chen, N. Cui, Q.Q. Wu, and Y.L. Su, Giant magneto impedance effect of Co-rich amorphous fibers under magnetic interaction, *Int. J. Miner. Metall. Mater.*, 27(2020), No. 10, p. 1415.

[5] M.V. Rane, V.H. Bafna, R. Sadanandam, A.K. Sharma, K. Ramadevi, N.K. Menon, M.F. Fonseca, S.K. Tangri, and A.K. Suri, Recovery of high purity cobalt from spent ammonia cracker catalyst, *Hydrometallurgy*, 77(2005), No. 3-4, p. 247.

[6] R.H. Matjie, M.M. Mdleleni, and M.S. Scurrell, Extraction of cobalt(II) from an ammonium nitrate-containing leach liquor by an ammonium salt of di(2-ethylhexyl)phosphoric acid, *Miner. Eng.*, 16(2003), No. 10, p. 1013.

[7] H. Setiawan, H.T.B.M. Petrus, and I. Perdana, Reaction kinetics modeling for lithium and cobalt recovery from spent lithium-ion batteries using acetic acid, *Int. J. Miner. Metall. Mater.*, 26(2019), No. 1, p. 98.

[8] J.P.T. Kapusta, Cobalt production and markets: A brief overview, *JOM*, 58(2006), No. 10, p. 33.

[9] C.Y. Feng and D.Q. Zhang, Cobalt deposits of China: Classification, distribution and major advances, *Acta. Geol. Sin.*, 78(2004), No. 2, p. 352.

[10] R.R. Moskalyk and A.M. Alfantazi, Review of present cobalt recovery practice, *Min. Metall. Explor.*, 17(2000), No. 4, p. 205.

[11] I.G. Sharma, P. Alex, A.C. Bidaye, and A.K. Suri, Electrowinning of cobalt from sulphate solutions, *Hydrometallurgy*, 80(2005), No. 1-2, p. 132.

[12] M.Z. Zhang, G.C. Zhu, Y.N. Zhao, and X.J. Feng, A study of recovery of copper and cobalt from copper-cobalt oxide ores by ammonium salt roasting, *Hydrometallurgy*, 129-130(2012), p. 140.

[13] M.C. Apua and A.F. Mulaba-Bafubiandi, Dissolution of oxidised Co - Cu ores using hydrochloric acid in the presence of ferrous chloride, *Hydrometallurgy*, 108(2011), No. 3-4, p. 233.

[14] B. Gupta, A. Deep, V. Singh, and S.N. Tandon, Recovery of cobalt, nickel, and copper from sea nodules by their extraction with alkylphosphines, *Hydrometallurgy*, 70(2003), No. 1-3, p. 121.

[15] Z.X. Liu, Z.L. Yin, S.F. Xiong, Y.G. Chen, and Q.Y. Chen, Leaching and kinetic modeling of calcareous bornite in ammonia ammonium sulfate solution with sodium persulfate, *Hydrometallurgy*, 144-145(2014), p. 86.

[16] Z.X. Liu, Z.L. Yin, H.P. Hu, and Q.Y. Chen, Leaching kinetics of low-grade copper ore containing calcium-magnesium carbonate in ammonia-ammonium sulfate solution with persulfate, *Trans. Nonferrous Met. Soc. China*, 22(2012), No. 11, p. 2822.

[17] A. Baba, M.K. Ghosh, S.R. Pradhan, D.S. Rao, A. Baral, and F.A. Adekola, Characterization and kinetic study on ammonia leaching of complex copper ore, *Trans. Nonferrous Met. Soc. China*, 24(2014), No. 5, p. 1587.

[18] Z.P. Zhao, M. Guo, and M. Zhang, Extraction of molybdenum and vanadium from the spent diesel exhaust catalyst by ammonia leaching method, *J. Hazard. Mater.*, 286(2015), p. 402.

[19] C. Wang, Y.F. Guo, S. Wang, F. Chen, Y.J. Tan, F.Q. Zheng, and L.Z. Yang, Characteristics of the reduction behavior of zinc ferrite and ammonia leaching after roasting, *Int. J. Miner. Metall. Mater.*, 27(2020), No. 1, p. 26.

[20] Y.M. Chen, N.N. Liu, F. Hu, L.G. Ye, Y. Xi, and S.H. Yang, Thermal treatment and ammoniacal leaching for the recovery of

valuable metals from spent lithium-ion batteries, *Waste. Manage.*, 75(2018), p. 469.
[21] C.B. Wu, B.S. Li, C.F. Yuan, S.N. Ni, and L.F. Li, Recycling valuable metals from spent lithium-ion batteries by ammonium sulfite-reduction ammonia leaching, *Waste. Manage.*, 93(2019), p. 153.
[22] Y.P. Qi, F.S. Meng, X.X. Yi, J.C. Shu, M.J. Chen, Z. Sun, S.H. Sun, and F.R. Xiu, A novel and efficient ammonia leaching method for recycling waste lithium ion batteries, *J. Cleaner Prod.*, 251(2020), p. 119665.
[23] O.O. Oluokun and I.O. Otunniyi, Kinetic analysis of Cu and Zn dissolution from printed circuit board physical processing dust under oxidative ammonia leaching, *Hydrometallurgy*, 193(2020), p. 105320.
[24] X.H. Meng and K.N. Han, The principles and applications of ammonia leaching of metals—A review, *Miner. Process. Extr. Metall. Rev.*, 16(1996), No. 1, p. 23.
[25] N. Peng, B. Peng, H. Liu, K. Xue, D. Chen, and D.H. Lin, Reductive roasting and ammonia leaching of high iron-bearing zinc calcines, *Miner. Process. Extr. Metall.*, 127(2018), No. 1, p. 1.
[26] S.W. Li, H.Y. Li, W.H. Chen, J.H. Peng, A.Y. Ma, S.H. Yin, L.B. Zhang, and K. Yang, Ammonia leaching of zinc from low-grade oxide zinc ores using the enhancement of the microwave irradiation, *Int. J. Chem. React. Eng.*, 16(2018), No. 3, art. No. 20170055.
[27] J.A. Dean, *Lange's Handbook of Chemistry*, 13th ed., Science Press, Beijing, 1991.
[28] Department of Analytical Chemistry, Central South Institute of Mining and Metallurgy, *Handbook of Chemical Analysis*, Science Press, Beijing, 1982.
[29] T. Nakamura, H. Kudo, Y. Tsuda, Y. Matsushima, and T. Yoshida. Electrodeposition of Zn–Co–Terephthalate MOF and Its Conversion to Co-Doped ZnO Thin Films, *ECS J. Solid State Sci.*, 10(2021), No. 5, art. No. 057002.
[30] J.H. Liu, H.R. Zhang, R.X. Wang, and T. Huang, Process of ammonium leaching oxidation ore of cobalt and copper at high pressure, *Chin. J. Rare Met.*, 36(2012), No. 1, p. 149.
[31] Y. Li, N. Kawashima, J. Li, A.P. Chandra, and A.R. Gerson, A review of the structure, and fundamental mechanisms and kinetics of the leaching of chalcopyrite, *Adv. Colloid Interface Sci.*, 197-198(2013), p. 1.
[32] A. Khawam and D.R. Flanagan, Solid-state kinetic models: Basics and mathematical fundamentals, *J. Phys. Chem. B.*, 110(2006), No. 35, p. 17315.
[33] X.J. Zhou, Y.L. Chen, J.G. Yin, W.T. Xia, X.L. Yuan, and X.Y. Xiang, Leaching kinetics of cobalt from the scraps of spent aerospace magnetic materials, *Waste. Manage.*, 76(2018), p. 663.
[34] C.H. Deng, Q.M. Feng, and Y. Chen, Studies on the leaching kinetics of cobalt from spent catalyst with sulphuric acid, *Miner. Process. Extr. Metall.*, 116(2007), No. 3, p. 159.
[35] L. Li, Y.F. Bian, X.X. Zhang, Y.B. Guan, E.S. Fan, F. Wu, and R.J. Chen, Process for recycling mixed-cathode materials from spent lithium-ion batteries and kinetics of leaching, *Waste. Manage.*, 71(2018), p. 362.